ELSEVIER

Ceramics International 27 (2001) 367–372

CERAMICS
INTERNATIONAL

www.elsevier.com/locate/ceramint

Electrical characterization of lead zirconate titanate prepared by organic solution route

Wanda C. Las *, Priscila D. Spagnol, Maria A. Zaghete, Mario Cilense

Instituto de Química, UNESP — C.P. 355, 14801-970, Araraquara, SP, Brazil

Received 22 December 1999; received in revised form 12 June 2000; accepted 15 June 2000

Dedicated to the memory of Professor Waldemar Saffioti.

Abstract

Two series of lead zirconate titanate (PZT) ceramics with composition Zr/Ti $\approx$ 53/47 have been prepared by the organic solution route. The effects on the electrical properties of calcination temperature in one series and of sintering time period in the other were examined. Dielectric constant, electrical conductivity and impedance spectroscopy results differed from one series to the other, probably due to differences in structure of the precursor powders, as seen by X-ray diffraction. Tetragonal and rhombohedral phases predominate in the powders used, respectively, in the calcined and sintered series. Physical and electrical behavior of ceramics prepared from predominantly rhombohedral powder suggests the evaporation of PbO. The presence of two semi-circles in impedance plots leads to the association of the low frequency semi-circle to the presence of PbO, which, apparently, was not eliminated from ceramics prepared from predominantly tetragonal powder. © 2001 Elsevier Science Ltd and Techna S.r.l. All rights reserved.

Keywords: C. Dielectric properties; C. Electrical conductivity; C. Impedance; D. PZT

1. Introduction

PZT can be obtained by conventional oxide mixture or synthesized by chemical processes including synthesis of organic solutions from citrates. This method has been introduced by Pechini [1] and produces a highly reactive powder as compared to the conventional one. PZT prepared by an oxide mixture may present chemical inhomogeneities as seen by several surface analysis techniques in pure and doped material [2]. Also, compositional fluctuations were seen in PZT ceramics prepared by oxide mixture as a function of calcination and sintering conditions using X-ray line-broadening analysis [3]; these fluctuations were also observed in PZT containing excess PbO [4].

The Pechini method, since starting from a more reactive powder, should yield better final properties as a result of an improved microstructure [5]. However, some steps in powder synthesis are important, such as calcining treatment, which can change phase composition [6] and affect the ceramics' electrical and dielectric properties. Impedance analysis has been applied to ionic conductors such as zirconia ceramics. For this material, it has been shown by Kleitz et al. [7,8] that a blocking effect exists caused sometimes by an impurity phase segregated at the boundary. They [8] mention that this blocking effect also appears in electronically conducting ceramics. Fleig and Maier [9] have shown that the existence of insulating gaps at the electrode/solid electrolyte interface results in two semicircles in the complex impedance plane. In this work, we present dielectric constant, electrical conductivity and impedance spectroscopy data related to powder characteristics for pure PZT prepared by Pechini's method and thermally treated at various calcining temperatures and sintering times. We show that two semicircles are present in PZT ceramics and suggest that the low frequency one, associated to the blocking effect, is related to a PbO phase remaining in the ceramics prepared from the predominantly tetragonal powder.

2. Experimental procedure

PZT powders were prepared from citrate precursors using a modified Pechini process, as described in detail elsewhere [6]. The composition was chosen near the

---

* Corresponding author. Fax: +55-16-222-7932.
E-mail addresses: wlas@iq.unesp.br (W.C. Las).

PII: S0272-8842(00)00089-4

morphotropic phase boundary region with Zr/Ti ≈ 53/47. Two batches were prepared, A and B. Batch A was divided in five portions, calcined, respectively, at 600, 650, 700, 750 and 800°C for 3 h. Batch B was all calcined at 600°C for 3 h followed by 700°C for 3 h. The second treatment was done because the first did not result in a good crystalline powder. Powders were characterized as to phase composition by X-ray diffraction analysis. Powders were uniaxially and isostatically pressed at 15 and 230 MPa, respectively, into discs ~ 3 mm thick and 8 mm in diameter. All discs from batch A were sintered at 1100°C for 6 h, while those from batch B were sintered at 1100°C for times ranging from 30 min to 8 h. Sintering was performed in a closed system, in a lead rich atmosphere set up by 15 wt.% of lead zirconate powder enriched with 5 wt.% PbO. Hereafter, ceramics from batch A will be referred to as calcined series and those from batch B, as sintered series. Apparent density was determined by the Archimedes method.

Energy dispersive spectroscopy (EDS) was carried out in a X-ray analyser series II Noran Instruments. In both series, an inner surface obtained by fracture was examined. The EDS was done at seven points distributed along two perpendicular axes on the whole fractured surface. Each data set was treated statistically by calculating the mean value, $\bar{x}$, and standard deviation, σ, of the EDS line intensities. A coefficient of variation, defined as $\sigma/\bar{x}\times100\%$, is then calculated and is a measure of the fluctuation in line intensity values. Although there was an overlapping of Pb–M and Zr–L lines in the low energy region, EDS results could be analyzed on comparative basis. Grain size was determined from microstructures obtained in a JEOL JSM T330A scanning electron microscope.

Ceramics were polished and ohmic contacts were made by applying silver paste (Degussa 200) to the ceramics parallel surfaces. Three types of electrical parameters were obtained as a function of temperature: (a) conductivity, by measuring resistance with a multimeter HP-3457 (internal impedance $10^{10}\Omega$); (b) dielectric constant, by measuring capacitance in an impedance analyser HP-4192 (oscillator amplitude = 50 mV); (c) real and imaginary impedance in the same impedance analyser.

3. Results and discussion

3.1. Powder characterization

Batches A and B of PZT powder, described in the experimental procedure, resulted in two different powders after calcination, as seen in the X-ray diffraction (XRD) pattern in Fig. 1. Batch A shows predominantly tetragonal structure (T) while batch B shows predominantly rhombohedral structure (R). It has been reported [4,10] that the coexistence region of both phases, R and T, in a sintered ceramics is a little over 1 at.%. Since powders A and B had different calcination treatments (700°C for powder A and 600°C plus 700°C for powder B), this could be the reason for the different XRD patterns. On the other hand, Soares et al. [11] reported that chemical equilibrium is not attained in PZT powders calcined at high temperatures (up to 1100°C) and for long periods. This suggests that a small variation in composition during preparation may result in the observed XRD different spectra.

3.2. Physical characterization of sintered ceramics

Mass variation was observed in ceramics weighed before and after sintering for both calcined and sintered

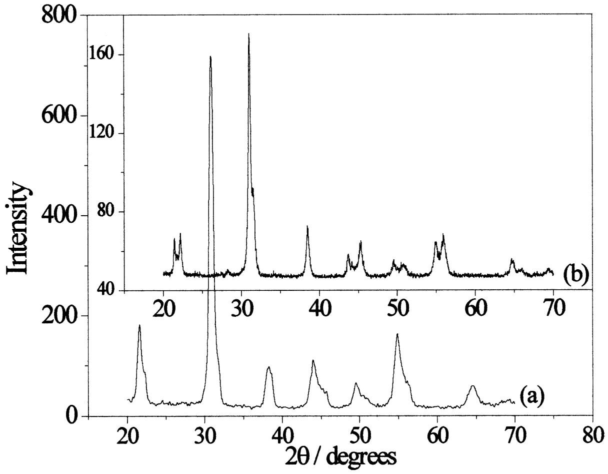

Fig. 1. X-ray diffraction of PZT powder from: (a) batch B (sintered series) calcined at 600°C/3 h and at 700°C/3 h, predominantly rhombohedral; (b) batch A (calcined series) calcined at 700°C/3 h, predominantly tetragonal.

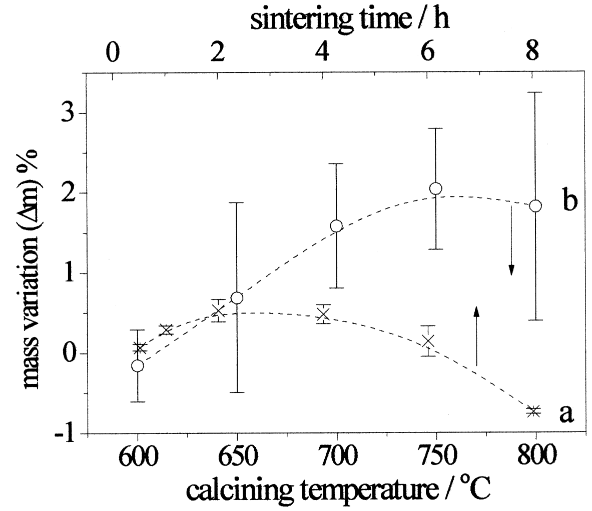

Fig. 2. Mass variation observed in PZT ceramics weighed before and after sintering: (a) sintered series (×); (b) calcined series (O).

series, as shown in Fig. 2. There is a mass gain in both cases which increases with increasing calcining temperature or sintering time, probably due to PbO incorporation in the grain boundaries. Mass gain decreases with prolonged treatment, probably due to PbO evaporation. For sintering time of 8 h a mass loss was observed. Also, mass variation is larger for the calcined series than for the sintered one. The standard deviation of three measurements, represented by the error bars, is much larger for the calcined series than for the sintered one.

Apparent density is shown in Fig. 3 for both series. It has low values for short sintering time periods, then increases due to elimination of pores and decreases for large periods due to PbO evaporation. For the calcined series it does not change much and decreases for high calcining temperatures. It has lower maximum apparent density than for the sintered series by 1.4%. Each experimental point is an average value of four measurements with a standard deviation $\leqslant$ 1%, and 2% for 800°C, as shown by the error bars.

Grain size increased with increasing sintering time period in the sintered series from $\sim$ 0.5 to $\sim$ 2 μm. Ceramics from both series, similarly treated (700°C/3 h and 1100°C/6 h), do not differ in grain size, around 1 μm.

Table 1 shows the coefficient of variation obtained from the analysis of the Pb, Zr and Ti EDS lines, for both series studied.

It is seen that the coefficient of variation, which we will call fluctuation, is larger for the calcined series than for the sintered one, a result that parallels that obtained for mass variation (Fig. 2). Also, for 800°C calcination this fluctuation is very large and may be related to the decrease in mass variation (Fig. 2), to the decrease in apparent density (Fig. 3) and to the increase in grain boundary resistivity (Table 2). It can also be noted that, at least for Pb, the fluctuation values for 6 h of sintering (near the best sintering condition) is the smallest. For 8 h sintering, however, the fluctuation values increase again while the ceramics density (Fig. 3) decreases.

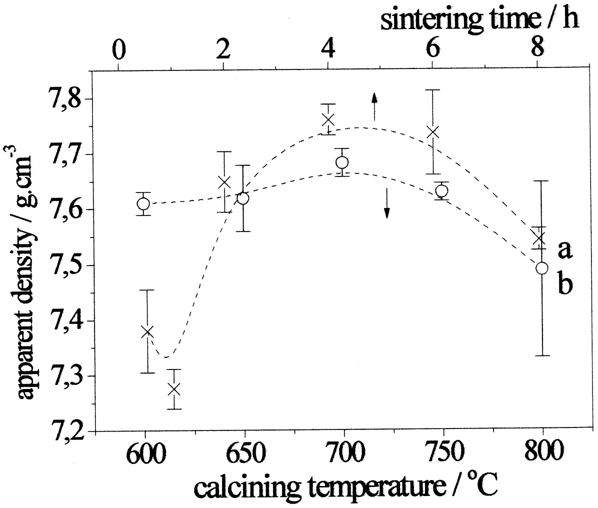

Fig. 3. Apparent density of sintered PZT: (a) sintered series (×); (b) calcined series (O).

3.3. Electrical characterization

Figs. 4 and 5 show results of dielectric constant as a function of temperature at 100 kHz. The Curie temperature, T_C, is equal to 420°C for the calcined series and 390°C for the sintered series. This difference, observed for equally treated ceramics (calcined at 700°C for 3 h and sintered at 1100°C for 6 h), suggests that the difference in powder composition (Fig. 1) persists even after sintering. The difference in T_C can be explained by the difference in powder composition, since the calcined series, with predominantly tetragonal structure, must be richer in lead titanate (PT) phase which has a higher T_C (490°C), while the sintered series, with predominantly rhombohedral structure, must be richer in lead zirconate (PZ) phase which has a lower T_C (233°C).

The dielectric constant at T_C, k_{max}, increases with calcination temperature and sintering time, except for 8 h sintering; it also shifts slightly towards lower temperatures with increasing calcination temperature. The increase in k_{max} could be the result of an improved microstructure and the increase in the apparent density, while the shift in k_{max} could be the consequence of a small change in composition, where the excess of PT phase would be consumed with increasing calcination temperature. We note that k_{max} for the sintered series is around twice the value for the calcined series. This result may be due to the difference in starting powders, with PbO evaporation occurring in the sintered series leading to an improved microstructure. This is also correlated to the conductivity results, as will be seen below.

In Fig. 6, the conductivities of two ceramics, from the sintered and calcined series are shown as a function of

Table 1
Coefficient of variation ($\sigma/\bar{x}\times100\%$) of EDS lines

T_{calc} (°C)	Zr–L (%)	Pb–M (%)	Ti–K (%)
a. Calcined series			
600	8.2	4.4	8.6
650	8.2	4.8	7.2
700	6.7	4.0	4.9
750	8.2	4.9	3.9
800	19.3	11.6	9.2
t_{sint} (h)	Zr–L (%)	Pb–M (%)	Ti–K (%)
b. Sintered series			
1	2.5	1.7	1.0
2	2.1	1.8	4.0
6	2.4	0.8	4.2
8	4.5	2.3	4.3

the inverse of temperature, for the best calcination plus sintering conditions. The observed behavior is similar for the other ceramics. The conductivity of the ceramics from the sintered series is higher than that of the calcined one, but changes in grain size and density alone do not account for the difference, suggesting that variation in Zr/Ti ratio is also important. The conductivity curves present two different slopes, one corresponding to the para-electric region and the other to the ferroelectric one; the temperature where there is a change in slope corresponds approximately to the Curie temperature. The activation energies in the para-electric and ferro-electric regions are, respectively, 0.77 and 1.1 eV for the calcined series and 0.90 and 1.1 eV for the sintered series. An activation energy of 0.71 eV has been reported [12] for PZT, calcined at 700°C for 1 h, sintered at 1200°C and measured between 500 and 700°C, and fitted by ($\Delta H_{ox}/2 + E_A + \Delta H_m/kT$), where the three energies correspond, respectively, to oxidation enthalpy, hole trapping energy and enthalpy of motion for holes. As these measurements were carried out above 500°C, the value of 0.71 eV corresponds to the para-electric region and is similar to the value found in the calcined series but lower than that for the sintered series. Although the sintering temperature and the measuring temperature range are not exactly the same in both works, the agreement of these energy values for the calcined series better than for the sintered one is thought to be a consequence of the composition variation we have in both series. The PZT studied in Raymond and Smyth's paper [12] has a Zr/Ti ratio of 50/50; if we remember that the calcined series has deviated from the intended 53/47 ratio to a composition richer in PT phase, as indicated by the XRD spectrum, then the

Table 2
Impedance fitting parameters of PZT bulk ferroelectric (bf) and grain boundary (gb) semicircles from (A) calcined series and (B) sintered series[a]

	ρ_{bf}	C_{bf}	f_{bf}	α_{bf}	ρ_{gb}	C_{gb}	f_{gb}	α_{gb}
	Ω/cm	10^{-10} F/cm	10^5 Hz		Ω/cm	10^{-9} F/cm	10^4 Hz	
A. Calcining temperature (°C)								
600	5500	2.60	1.09	0.0665	16 440	0.67	1.45	0.2500
650	4842	2.65	1.22	0.0569	11 107	0.72	1.98	0.2395
700	4345	2.81	1.29	0.0645	8619	0.97	1.91	0.2513
750	3952	2.92	1.37	0.0850	3913	1.83	2.21	0.2208
800	5019	2.85	1.10	0.1022	9257	1.51	1.14	0.2459
B. Sintering time (h)								
2	5228	1.45	2.09	0.0525	1486	6.16	1.74	0.2336
6	3036	2.03	2.58	0.0467	679	16.9	1.39	0.2657
8	3374	2.18	2.15	0.0723	976	9.67	1.68	0.2849

[a] Temperature of measurement, 484°C.

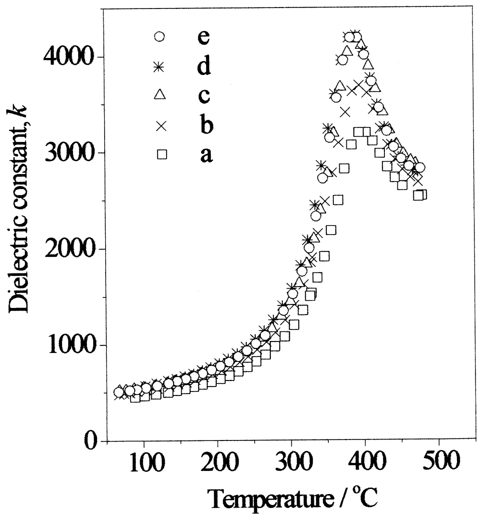

Fig. 4. PZT calcined at: (a) 600°C; (b) 650°C; (c) 700°C; (d) 750°C and (e) 800°C for 3 h and sintered at 1100°C for 6 h, measured at 100 kHz.

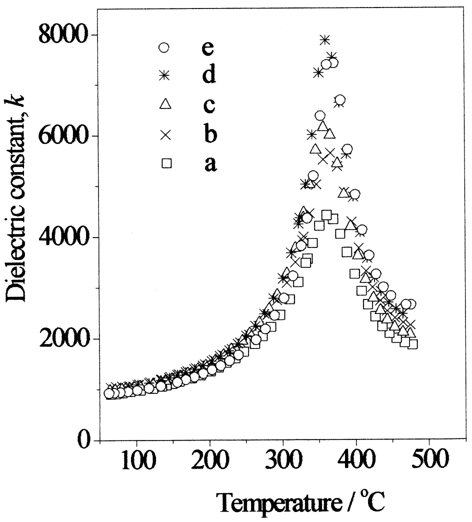

Fig. 5. PZT calcined at 700°C for 3 h and sintered at 1100°C for: (a) 30 min; (b) 2 h; (c) 4 h; (d) 6 h and (e) 8 h, measured at 100 kHz.

agreement with the calcined series and not with the sintered one can be explained. Also, our conductivity values are somewhat lower than in that paper, as expected, since it is known that lower sintering temperatures decrease the material conductivity. The activation energy in the ferro-electric region being higher than in the para-electric one indicates that the hole conduction is energetically less favorable when the domains are oriented.

Fig. 7 shows complex impedance plots for both series. The curves were fitted by two semi-circles, the high frequency one corresponding to the bulk ferro-electric (bf) and the low frequency one corresponding to the grain boundary (gb) [13]. Parameter values, listed in Table 2, lead to various comparisons. The grain boundary resistivity, ρ_{gb}, decreases with increasing calcination temperature, while that of the bulk ferro-electric, ρ_{bf}, does not change so much. Also, C_{gb} increases with increasing calcination temperature, while C_{bf} does not change so much. The depression angle, α_{gb}, is large and α_{bf} is small, as one might expect, since this parameter is interpreted as a measure of material heterogeneity. In the sintered series, ρ_{gb} is much lower than in the calcined series, while ρ_{bf} is similar. The behavior of these parameters suggests that by increasing calcination temperature and sintering time the microstructure is improved, since grain boundary electrical characteristics are more affected than bulk properties. Although ρ_{bf} and C_{bf} do not vary from one series to the other as much as ρ_{gb} and C_{gb} do, the difference by a factor of two in $f_{bf} = 1/(2\pi R_{bf} C_{bf})$ could imply that slightly different bulk compositions resulted in both cases, probably because of the mentioned difference in powder composition. The fact that the low frequency semicircle is much smaller in the sintered series, for which k_{max} is higher, seems to indicate that its presence is related to a better microstructure.

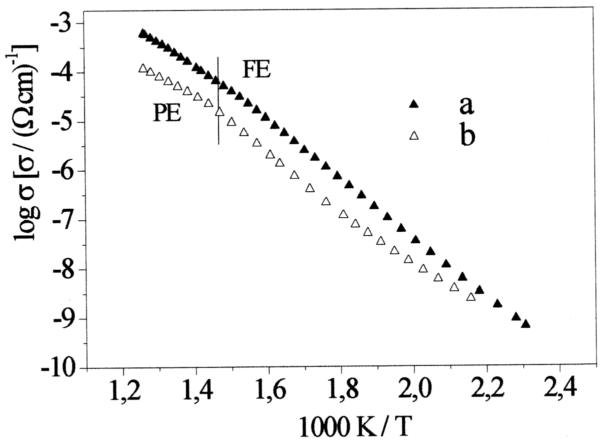

Fig. 6. Electrical conductivity of PZT calcined at 700°C for 3 h and sintered at 1100°C for 6 h; (a) sintered series and (b) calcined series (PE, para-electric phase; FE, ferro-electric phase).

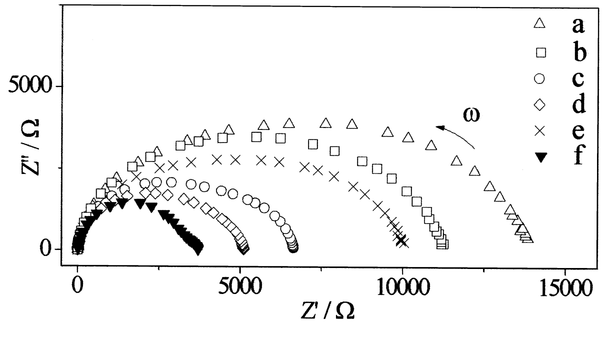

Fig. 7. Impedance plots of PZT calcined at: (a) 600°C; (b) 650°C; (c) 700°C; (d) 750°C; (e) 800°C for 3 h and sintered at 1100°C for 6 h (calcined series); (f) calcined at 600 and 700°C for 3 h and sintered at 1100°C for 6 h (sintered series) (temperature of measurement, 484°C).

4. Conclusions

It is possible to affirm that equal sintering conditions used for ceramic compacts obtained from similarly prepared powders (Zr/Ti ≈ 53/47), but which resulted in different phase composition, are not sufficient to obtain equal electrical properties. Indeed, electrical measurements revealed that differences in powder characteristics such as phase composition, can affect the ceramics final electrical properties. It is known that electrical measurements are very sensitive and, therefore, able to detect small changes in ceramics microstructure, which are not detected by microscopy analysis or apparent density measurements. Although treated statistically, EDS analysis together with mass variation may be helpful in interpreting electrical characterization results. It is suggested that the blocking effect, represented by the presence of the low frequency semi-circle, is due to PbO, which may have evaporated in the predominantly rhombohedral powder, but stayed in the predominantly tetragonal one.

Acknowledgements

We thank for financial support from FINEP/PADCT project no. 54.91.0231.00, FAPESP and CNPq.

References

[1] M.P. Pechini, Method of preparing lead and alkaline earth titanates and niobates and coating method using the same to form a capacitor. US Patent 3 330 697, 1967.

[2] M. Hammer, M.J. Hoffmann, B. Baretzky, Characterization of chemical inhomogeneities in doped and undoped PZT-ceramics, in: J.L. Baptista, J.A. Labrincha, P.M. Vilarinho (Eds.), Electroceramics V, 1996, University of Aveiro, Portugal. Proceedings. European Ceramic Society, Vol. I, pp. 161–164.

[3] S.K. Saha, D.C. Agrawal, Composition fluctuations and their

influence on the properties of lead zirconate titanate ceramics, Am. Ceram. Soc. Bull. 71 (9) (1992) 1424–1928.

[4] K. Kakegawa, O. Matsunaga, T. Kato, Y. Sasaki, Compositional change and compositional fluctuation in Pb(Zr,Ti)O_3 containing excess PbO, J. Am. Ceram. Soc. 78 (4) (1995) 1071–1075.

[5] M.A. Zaghete, J.A. Varela, M. Cilense, C.O. Paiva-Santos, W.C. Longo, E. Longo, The effect of isostructural seeding on the microstructure and piezoelectric properties of PZT ceramics, Ceram. Int. 25 (1999) 239–244.

[6] M.A. Zaghete, C.O. Paiva-Santos, J.A. Varela, E. Longo, Y.P. Mascarenhas, Phase characterization of lead zirconate titanate obtained from organic solutions of citrates, J. Am. Ceram. Soc. 75 (8) (1992) 2088–2093.

[7] M. Kleitz, H. Bernard, E. Fernandez, E. Schouler, Impedance spectroscopy and electrical resistance measurements on stabilized zirconia, in: Advances in Ceramics, Vol. 3, Science and Technology of Zirconia, The American Ceramic Society, 1981, pp. 310–336.

[8] M. Kleitz, L. Dessemond, M.C. Steil, Model for ion-blocking at internal interfaces in zirconias, Solid State Ionics 75 (1995) 107–115.

[9] J. Fleig, J. Maier, Finite element calculations of impedance effects at point contacts, Electrochim. Acta 41 (7/8) (1996) 1003–1009.

[10] H.-W. Wang, D.A. Hall, F. Sale, Phase homogeneity and segregation in PZT powders prepared by thermal decomposition of metal–EDTA complexes derived from nitrate and chloride solutions, J. Am. Ceram. Soc. 75 (1) (1992) 124–130.

[11] M.R. Soares, A.M.R. Senos, P.Q. Mantas, Phase coexistence in PZT ceramics, J. Eur. Ceram. Soc. 19 (1999) 1865–1871.

[12] M.V. Raymond, D.M. Smyth, Defect chemistry and transport properties of $Pb(Zr_{1/2}Ti_{1/2})O_3$, Integrated Ferroelectrics 4 (1994) 145–154.

[13] J.G. Fletcher, A.R. West, J.T.S. Irvine, The ac impedance response of the physical interface between yttria-stabilized zirconia and $YBa_2Cu_3O_{7-x}$, J. Electrochem. Soc. 142 (8) (1995) 2650–2654.